



Evaluation of the Efficacy of a Novel Injectable Hydrogel Containing Quercetin and Silver Nanoparticles to Enhance Bone Formation

Joshua Narde¹, Subhabrata Maiti¹, Karthik Ganesh Mohanraj², Jessy Paulraj³, Diana Russo⁴, Maria Maddalena Marrapodi⁵, Marco Cicciù⁶ and Giuseppe Minervini^{4,*}

¹Department of Prosthodontics, Saveetha Dental College and Hospital, Saveetha Institute of Medical and Technical Sciences, Saveetha University, Chennai, India

²Biomedical Research Unit and Lab Animal Centre (BRULAC), Saveetha Dental College and Hospitals Saveetha Institute of Medical and Technical Sciences, Saveetha University Chennai-600077, Tamilnadu, India

³Department of Pedodontics, Saveetha Dental College and Hospital, Saveetha Institute of Medical and Technical Sciences, Saveetha University, Chennai, India

⁴Multidisciplinary Department of Medical-Surgical and Odontostomatological Specialties, University of Campania "Luigi Vanvitelli", 80121 Naples, Italy

⁵Department of Woman, Child and General and Specialist Surgery, University of Campania "Luigi Vanvitelli" Naples

⁶Department of Biomedical and Surgical and Biomedical Sciences, Catania University, 95123, Catania, Italy

Abstract:

Aim: This study aimed to ascertain the efficacy of a novel injectable hydrogel containing quercetin and silver nanoparticles incorporated with gelatin to enhance bone formation.

Materials and Methods: The lyophilized material preparation involved creating a gel-based medium containing xenogenic bone graft Bio-Oss, silver nanoparticles, and quercetin, followed by freeze-drying and injection into rat femurs for antibacterial efficacy and structural property assessment via an MTT Assay. *In vitro* analysis included testing cell viability and antimicrobial properties. Swelling tests measured scaffold swelling ratios in a culture medium, providing insights into their performance. Animal studies were conducted involving surgical procedures to create bone defects and assess the efficacy of bone grafts on rat tibiae. Nano-computed tomographic imaging was used to evaluate changes in bone volume post-operation, providing detailed insights into alterations in trabecular content. An independent t-test was performed for statistical analysis.

Results: No significant difference was found between groups with respect to cell viability and antimicrobial activity. There was maximum bone volume and trabecular width seen in the experimental group ($426.54 \pm 34.78 \text{ mm}^3$, $0.509 \pm 0.023 \text{ mm}$), followed by the control group, and the difference was statistically significant ($p < 0.05$).

Conclusion: The study shows that the application of this injectable hydrogel helped in enhancing bone formation.

Keywords: Injectable hydrogel, Bone grafts, Silver nanoparticles, Bone augmentation, Atrophic ridges.

© 2025 The Author(s). Published by Bentham Open.

This is an open access article distributed under the terms of the Creative Commons Attribution 4.0 International Public License (CC-BY 4.0), a copy of which is available at: <https://creativecommons.org/licenses/by/4.0/legalcode>. This license permits unrestricted use, distribution, and reproduction in any medium, provided the original author and source are credited.

*Address correspondence to this author at the Multidisciplinary Department of Medical-Surgical and Odontostomatological Specialties, University of Campania "Luigi Vanvitelli", 80121 Naples, Italy; E-mail: minerviniigiuseppe@hotmail.it

Cite as: Narde J, Maiti S, Mohanraj K, Paulraj J, Russo D, Marrapodi M, Cicciù M, Minervini G. Evaluation of the Efficacy of a Novel Injectable Hydrogel Containing Quercetin and Silver Nanoparticles to Enhance Bone Formation. Open Dent J, 2025; 19: e18742106348783. <http://dx.doi.org/10.2174/0118742106348783250515114241>



CrossMark

Received: October 01, 2024

Revised: January 27, 2025

Accepted: April 04, 2025

Published: May 16, 2025



Send Orders for Reprints to
reprints@benthamscience.net

1. INTRODUCTION

Atrophic alveolar ridges are a common issue, posing significant challenges for both patients and practitioners. These ridges are characterized by a reduction in the volume of the maxilla and mandible, which can be caused by periodontal disease, endodontic complications, or trauma, eventually leading to tooth loss due to vertical or horizontal bone loss. This bone resorption can result in a variety of issues, including decreased oral function, aesthetic concerns, and difficulties in dental implant placement and restoration. Bone grafting has emerged as a crucial and effective solution to address these problems. In this treatment modality, bone graft material is used to supplement areas of deficient bone, helping to restore a solid foundation for dental prostheses and implants.

A bone graft is a crucial tissue that can promote bone healing when implanted into a bony defect, either alone or in combination with other materials [1]. Bone graft materials can vary, with autogenous grafts being harvested from the patient's own body. Common sources for autogenous grafts include intraoral sites such as the ramus of the mandible and symphysis, as well as extraoral sites like the fibula and iliac crest [2, 3]. Allografts, on the other hand, are materials obtained from a donor of the same species [4]. Some of the most commonly used bone grafts available commercially include Demineralized Freeze-Dried Bone Allografts (DFDBAs) and Freeze-Dried Bone Allografts (FDBAs) [5]. Xenografts are materials that are procured from different species altogether. They could be of bovine or porcine origin [6]. Alloplastic grafts are made of synthetic materials like hydroxyapatite or bioactive glass.

Dental implants require a strong and healthy bone for osseointegration, which is the main reason why bone grafting is necessary in scenarios where bony defects or atrophic ridges are present. The implants act as artificial tooth roots, and in order for osseointegration to occur, there must be enough bone density and volume, keeping in mind that there is a chance resorption could occur [7]. The lack of healthy bone could result in issues, such as implant instability, pain, or, in worse cases, even implant rejection. Dental specialists can strengthen and rejuvenate the weakened bone through bone grafting operations, providing a stable foundation for implant placement. Various studies have shown the importance and increased frequency of the usage of grafting procedures [8, 9].

Xenogeneic bone grafts are commonly used to augment areas of the alveolar ridges that lack sufficient width or height, preparing these regions for dental implants. These grafts undergo specific treatments to minimize the risk of immunological reactions and disease transmission. Generally, xenogeneic bone grafts have demonstrated good success rates [10]. They provide a biocompatible scaffold that facilitates the development and integration of new bone, creating a stable foundation for dental implants. Xenogeneic bone grafts have proven effective in facilitating implant insertion and promoting long-term dental health outcomes. However, success rates may vary based on patient-specific factors and grafting techniques. These grafts are available in various forms, such as powder and putty, and the use of resorbable and non-resorbable mem-

branes, including titanium membranes, can further enhance long-term success [11, 12].

Injectable hydrogels represent a promising new category of xenogeneic bone solutions. With high biocompatibility, predictable application, and customizable properties, hydrogel systems enable minimally invasive surgeries without the need for subsequent implant procedures. Additionally, they provide effective methods for mimicking the Extracellular Matrix (ECM) and encapsulating a variety of mesenchymal stem cells and bioactive substances. This approach helps to fill the defect zone and promotes bone growth [13].

The above benefits enable hydrogel systems to satisfy the unique requirements of repair and regeneration. This study was conducted to ascertain the success of a novel injectable hydrogel containing quercetin and silver nanoparticles incorporated with gelatin to enhance bone formation, where the null hypothesis stated that there would be no change in the bone formation after the addition of a gelatin-based injectable hydrogel.

2. MATERIALS AND METHODS

2.1. Study Design

The sample size for the study was decided using the G-Power software (Version 3.1.9). The final calculation indicated that 16 samples should be included [13]. The animal ethical clearance was also obtained from the Institutional Animal Ethics Committee (IAEC), Biomedical Research Unit and Laboratory Animal Centre at Saveetha Dental College and Hospital, Saveetha Institute of Medical and Technical Sciences, Chennai, India (BRULAC/SDCH/SIMATS/IAEC/05-2022/118).

2.2. Hydrogel Preparation Protocol

About 10% (w/v) gelatin solution was prepared by dissolving Gelatin Type B (Sigma-Aldrich, USA) in distilled water under continuous stirring at 50°C. Methacrylation was carried out by gradually adding methacrylic acid (20:1 molar ratio to gelatin) while stirring at room temperature. Xenogenic bone graft (Bio-Oss, Geistlich, Switzerland), silver nanoparticles, and quercetin were then introduced in precise quantities and stirred at 500 rpm for 30 minutes. Irgacure 2959 (0.5% w/v) was added, and stirring was continued for an additional 15 minutes under dark conditions. Crosslinking was initiated by exposing the hydrogel to 365 nm UV light for 10 minutes. The hydrogel was then frozen at -80°C overnight and lyophilized through freeze-drying for 48 hours to obtain the final lyophilized form. Finally, the hydrogel was sterilized and stored under vacuum-sealed conditions at room temperature until further use.

2.3. In-vitro Analysis

2.3.1. Cell Viability

Cell viability was assessed using the MTT assay [14]. A 1 mg/mL quercetin solution was added to the silver nanoparticle sample preparation, which was then immersed in Dulbecco's Modified Eagle Medium (DMEM F12). The medium contained 1% penicillin and 10% fetal bovine serum

(FBS) (Gibco, Waltham, USA). After incubation for 24 hours, the media was removed and replaced with fresh media for cell treatment to assess compatibility. The cells were further incubated for 24 hours, after which 10 μ L/100 mL of MTT reagent (5 mg/mL stock) was added. The cells were incubated for 4 hours at 37°C to allow formazan dye formation. The medium was then replaced with 200 μ L of Dimethyl Sulfoxide (DMSO) (Sigma-Aldrich, St. Louis, USA) and incubated for 10 minutes. The final reaction was transferred to a 96-well ELISA plate, and absorbance was measured at A570 using a plate reader.

2.3.2. Antimicrobial Test

Utilizing a sterile 5ml pipette, 5ml of sterile saline was meticulously introduced into a test tube, ensuring strict adherence to sterility protocols. *S. aureus* and *Candida albican* colonies were carefully chosen from subculture plates using sterile inoculating loops and transferred to distinct sterile saline tubes. Subsequently, the organisms underwent dilution to attain a turbidity mirroring the 0.5 McFarland standard. Post-dilution, a sterile swab was immersed in the inoculum, allowing absorption for a duration of 15 minutes. Excess fluid was eliminated by spinning the swab against the tube's inner wall.

The swab was used to streak the entire agar surface three times, rotating the plate and swab by 60 degrees between each streak. Drug-impregnated disks were then placed on the agar surface, and the plate was inverted for incubation at 37°C. *Streptococcus* organisms were incubated in an environment enriched with 5–10% CO₂. After an incubation period of 16–24 hours, only the areas exhibiting complete inhibition were measured in millimeters. These measurements were compared to those on the Disk Diffusion Zone Diameter Chart to determine antibiotic susceptibility based on the MIC concentrations, and continuous metric diameter tests were conducted.

2.3.3. Swelling Test

Measurements of the swelling ratio of the scaffolds were conducted in a culture medium maintained at 37°C. An electronic balance was utilized to accurately measure and record their initial weights. Subsequently, the scaffold samples were allowed to remain in the medium to swell for a complete day. Following this incubation period, the swollen scaffolds were removed from the medium and weighed, with any excess surface-adhered medium being gently wiped off using tissue paper. The swelling ratio was calculated using the formula: Swelling ratio = $(W_t - W_0) / W_0 \times 100\%$, where W_t represents the weight of the scaffold after immersion for a specified time 't' in the medium, and W_0 denotes the initial weight of the scaffold prior to immersion in the medium [15].

2.4. Animal Study

2.4.1. Sample Selection for Animal Study

The Animal Ethics Committee had approved all procedures involving the use of animals for this research. The lateral femoral shaft of a rat was fixed to be the ideal site for the test to be conducted, and a cylindrical bone defect

repair model was created. Sixteen male white Wistar albino rats, with an average weight of $296 \text{ g} \pm 25.6 \text{ g}$, were part of the test, all of whom were 3 to 5 months old. All animals used in this study were obtained from the Biomedical Research Unit and Laboratory Animal Centre, Saveetha Dental College and Hospitals, Saveetha Institute of Medical and Technical Sciences -SIMATS (CCSEA Registered In-House Breeding Approval Number: 856/PO/ReBi/S/04/CCSEA). The procured rats were housed and handled in accordance with the CCSEA (Committee for Control and Supervision of Experiments on Animals) guidelines. All the protocols were approved by the Institutional Animal Ethics Committee and followed strictly during the course of the experiment.

2.4.2. Estimation of Sample Size and Grouping

There were two experimental groups: the experimental group, which received the novel hydrogel-based bone graft, and the control group, which did not receive the hydrogel and served as a baseline to assess bone formation after implant placement. A total of 16 samples were included in the study.

2.4.3. Surgical Procedure

Under completely sterile circumstances, the surgery was conducted using an intraperitoneal injection of 2% xylazine (10 mg/kg) (Rompun, Bayer, Germany) and ketamine (10 mg/kg) Anaket, Neon Laboratories Ltd., India) to anesthetize the rats. Subcutaneous injections of buprenorphine were used for the reduction of postoperative pain. Keeping the knee joint fixed at full extension, the right hind limb was shaved. The lateral femoral condyle was exposed by a 15 mm longitudinal incision made lateral to the patellar ligament. Drilling with a 3 mm drill bit created a hole that was 4 mm deep and 3 mm in diameter. The broken bone chips were then removed with saline. To this, the gelatin-based bone graft material was added. The bone graft material was packed, and the excess was removed. The incision was sutured layer by layer to prevent the formation of any scar tissue after the surgical site was cleaned with regular saline. After six weeks, the rats were decapitated in order to remove their femurs (Fig. 1).

2.4.4. Histopathological Analysis

The implant placement site and surrounding tissue were removed, fixed in 10% neutral buffered formalin, and examined under a microscope. Following fixation, Hematoxylin & Eosin (H&E) stain was used to prepare tissue specimens.

2.4.5. Nano-computed Tomographic Imaging

Nano-computed tomographic scanning was employed to evaluate changes in bone volume in both experimental groups. The scanning was performed using a Nano-CT scanner (Skyscan 2214, Bruker, Billerica, USA), which provided detailed images of the bone slices. The obtained sections were reconstructed, and the grayscale images were analyzed. This allowed for a more accurate assessment of changes in trabecular content, aiding in the evaluation of the efficacy of the bone graft medium.

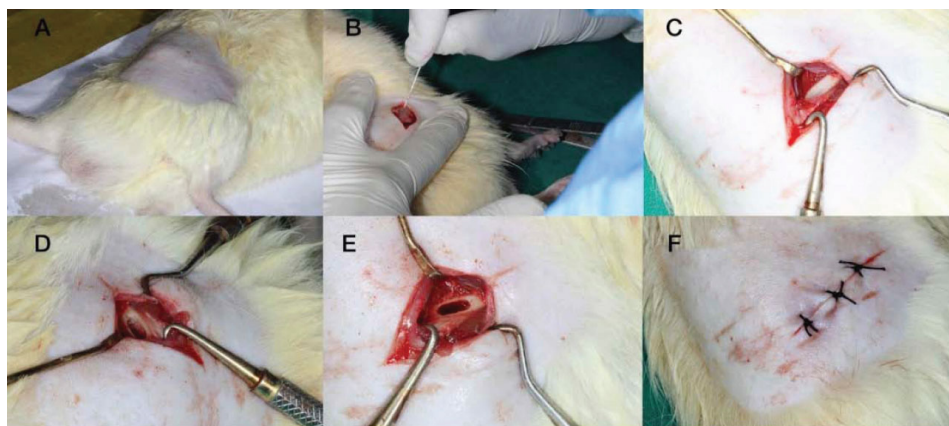


Fig. (1). (A)- Shaved site (B)- Incision, (C)- Elevation, (D)-Drilling protocol, (E)- Reflected site to receive the test gel, (F)- Suturing done.

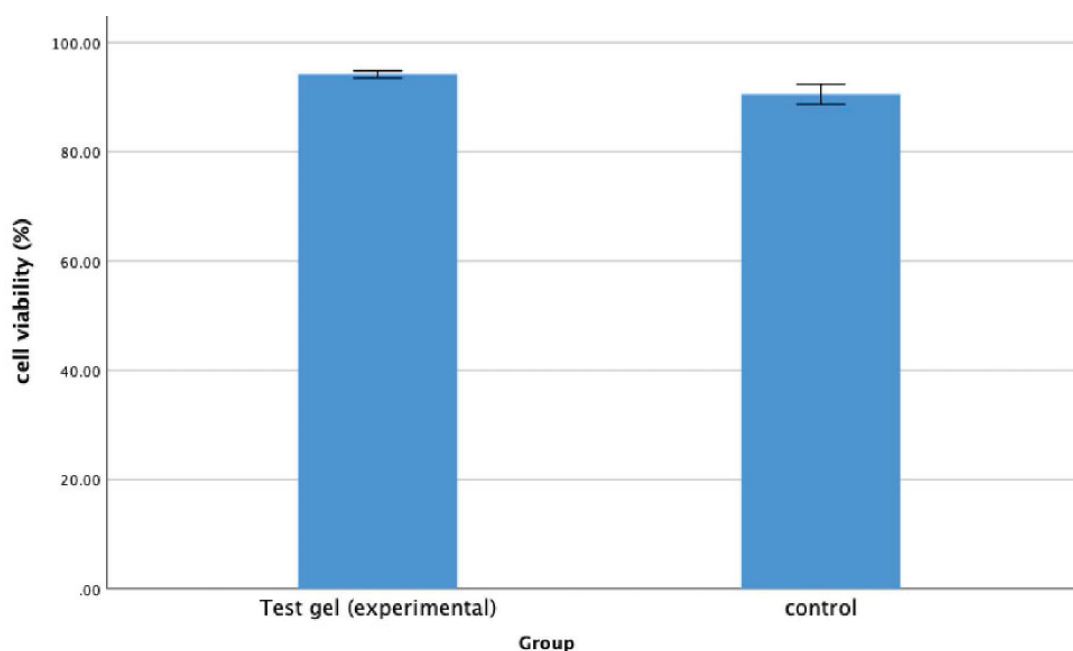


Fig. (2). Graphical representation of the cell compatibility between the control group and test gel.

2.5. Statistical Analysis

Statistical analysis was carried out using SPSS software (IBM Corp., 2011; IBM SPSS Statistics for Windows, Version 20.0; Armonk, NY: IBM Corp.), with a significance level established at $p < 0.05$ for all analyses. An Independent t-test was performed to compare the two groups.

3. RESULTS

3.1. Cell Compatibility

The purpose of this test was to determine whether the injectable hydrogel would be compatible with the surrounding cells at the site of placement. Compatibility is essential

for displaying osteogenic potential, which aids in bone formation. The cell compatibility tests revealed that the experimental gel exhibited good cell compatibility (92.16 ± 4.21) compared to the control group (90.50 ± 4.51). No significant difference was observed between the groups ($p=0.64$) (Fig. 2).

3.2. Antimicrobial Tests

The antimicrobial tests were conducted using *S. aureus* and *C. albicans*. The results demonstrated promising outcomes, with the experimental group showing a larger zone of inhibition for both organisms. However, no significant difference ($p>0.05$) was observed between the two materials tested (Table 1).

Table 1. Mean and standard deviation zone of inhibition on *C. Albicans* and *S. Aureus* for control and experimental group; *p*-value was derived from independent t test.

Dependent Variable	Group	Mean \pm SD	Mean Difference	T-value	<i>p</i> -value	Null Hypothesis
<i>S. Aureus</i>	Experimental group	32.12 \pm 0.64	0.62	1.81	0.09	Accepted
Control group	31.50 \pm 0.54					
<i>C. Albicans</i>	Experimental group	12.5 \pm 0.53	0.72	2.12	0.06	Accepted
Control group	11.78 \pm 0.64					

3.3. Histopathological Analysis

Histopathological evaluation revealed the defect area (indicated by asterisks) between the two-shaft walls of the femur bone in both the control and experimental groups. The femur walls consisted of compact bone (denoted by thin black arrows) maintaining its regular architecture. Material particles within the defect area were indicated by thick red arrows. The formation of a network of woven bone (depicted by thick black arrows) suggested the presence of immature bone at the defect site, demonstrating the ongoing process of bone remodeling and the subsequent transformation and maturation of endochondral ossification (Figs. 3 & 4).

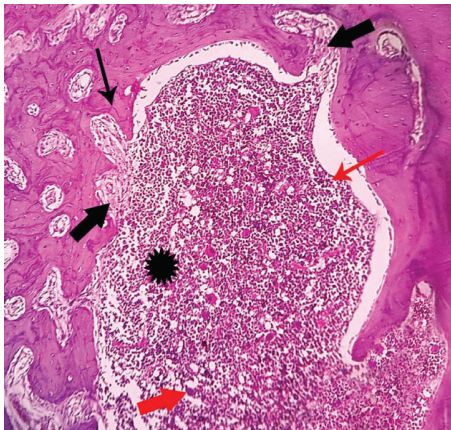


Fig. (3). Photomicrographs showing the histopathology of the control group stained with H&E at 10X Magnification.

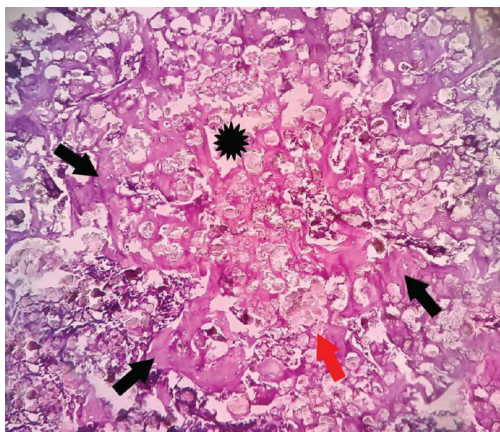


Fig. (4). Photomicrographs showing the histopathology of the experimental group stained with H&E at 10X Magnification.

3.4. Tomography Image

Nano-CT imaging revealed significant bone volume growth, and the data obtained from the imaging were used for the quantitative analysis of bone volume and trabecular width at the defect site 4 weeks postoperatively (Figs. 5 & 6). The experimental group showed the highest bone volume and trabecular width ($426.54 \pm 34.78 \text{ mm}^3$, $0.509 \pm 0.023 \text{ mm}$), followed by the control group ($281.93 \pm 17.59 \text{ mm}^3$, $0.415 \pm 0.042 \text{ mm}$). The differences between the groups for both parameters were statistically significant ($p < 0.05$) (Table 2).

4. DISCUSSION

The emergence of injectable hydrogels, highlighted as a promising advancement in xenogenic bone solutions [16, 17], presents a transformative approach to addressing widespread challenges associated with atrophic dental ridges [18]. Injectable hydrogels simulate the Extracellular Matrix (ECM), encapsulating mesenchymal stem cells and bioactive substances to foster bone growth [19, 20]. In the context of the study, the aim was to specifically target the enhancement of bone formation as a solution to the prevalent challenges posed by atrophic dental ridges given in the literature [21].

The comprehensive evaluation of this study reveals promising outcomes across multiple parameters. In the MTT assay, the treatment group exhibited notably higher cell viability compared to the control group, indicating the enhanced cellular compatibility of this developed formulation. Moreover, the antimicrobial test displayed the remarkable effectiveness of the presented material in comparison to the control group, highlighting its potential in combating microbial threats. AgNPs exhibit broad-spectrum antimicrobial properties, disrupting bacterial cell walls, inhibiting biofilm formation, and preventing post-surgical infections. Quercetin acts as an antibacterial agent by generating Reactive Oxygen Species (ROS) and impairing bacterial DNA (Deoxyribonucleic acid) replication, further enhancing wound healing. This explanation will clarify the biological role of these components in bone regeneration. Contrarily, in the swelling test, our treatment demonstrated reduced swelling compared to the control group, suggesting its ability to mitigate inflammation. Moving to the animal study, tomography imaging revealed distinctive patterns between the treatment group and the control group. The treatment group displayed favorable bone volume, indicating a pronounced potential for enhanced bone formation. Trabecular thickness provided insights into improved structural integrity. Quercetin has been shown to enhance osteoblastic differentiation by upregulating osteogenic

markers, such as ALP (Alkaline phosphatase), Runx2 (Runx-related transcription factor 2), and OCN (Osteocalcin). It activates the Wnt/ β -catenin and BMP (Bone Morphogenetic Proteins) signaling pathways, which play critical roles in bone formation. Silver nanoparticles (AgNPs) contribute to osteogenesis by promoting mesenchymal stem cell differentiation into osteoblasts and stimulating calcium depo-

sition. Quercetin enhances angiogenesis by increasing VEGF (Vascular endothelial growth factor) expression, which is essential for vascularization in bone healing. This supports nutrient supply and bone remodeling. AgNPs also play a role in angiogenesis by modulating endothelial cell proliferation and migration, aiding in neovascularization within the bone defect.

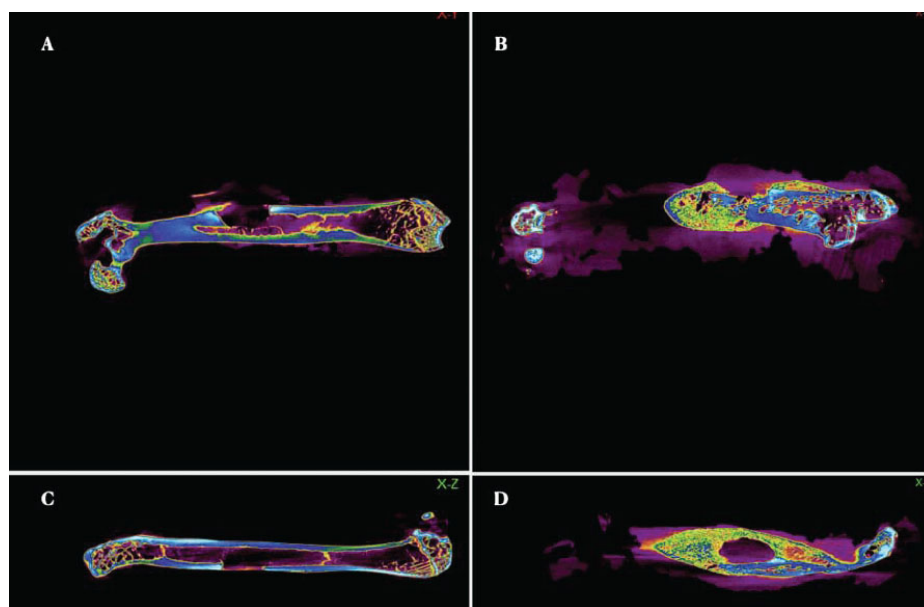


Fig. (5). Colour-enhanced 2D Nano CT images. The warm colours represent denser regions, while the cool colours indicate areas with less density. (A). Control group in the X-Y axis. (B). Experimental group in the X-Y axis. (C). Control group in the X-Z axis. (D). Experimental group in the X-Z axis.

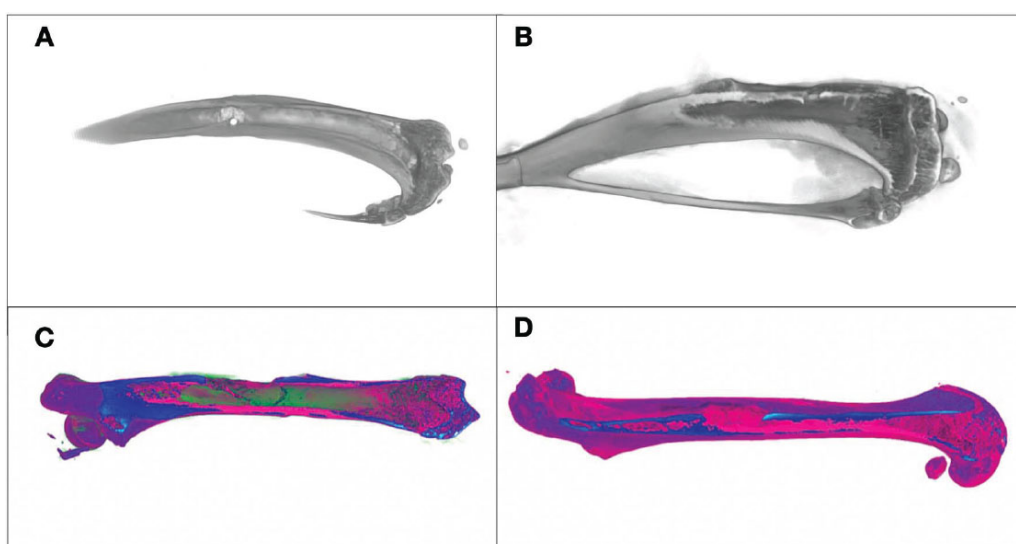


Fig. (6). Three-dimensional Nano CT views. (A). Control group (grayscale image), with bright areas indicating higher density and dark areas indicating lower density. (B). Experimental group (grayscale image) with similar density representation. (C). Control group (colour-enhanced image), where warm colours indicate denser regions and cool colours show less dense areas. (D). Experimental group (colour-enhanced image), with the same colour-coding indicating density variations.

Table 2. Mean and standard deviation of the bone volume and trabecular thickness of the experimental and control group; *p*-value was derived from independent t test.

Dependent Variable	Group	Mean \pm SD	Mean Difference	T-value	<i>p</i> -value	Null Hypothesis
Bone volume	Experimental group	426.54 \pm 34.78	144.60	3.19	0.006*	Rejected
	Control group	281.93 \pm 17.59				
Trabecular Thickness	Experimental group	0.509 \pm 0.023	0.09	4.77	0.001*	Rejected
	Control group	0.415 \pm 0.042				

The study stands in close relation to several key aspects of previous literature, solidifying its significance within the broader context of bone regeneration and biomaterial development [22]. Previous articles underscore the relevance of silver nanoparticles and gelatin in wound healing and osteogenic differentiation, yet our study advances beyond by combining these components synergistically. The MTT assay results underscore the effectiveness of our treatment, revealing significantly higher cell viability in the positive treatment group compared to the control. This supports the non-toxic nature of AgNPs/Gel hydrogels to osteoblasts, aligning with the findings of Han *et al.*, which explored the role of gelatin in stabilizing silver nanoparticles for bone fracture healing. Their study provides valuable insight into the individual components we integrate into our gelatin-based hydrogel [23]. By building on this understanding, our study advances the field by synergistically combining gelatin, quercetin, and silver nanoparticles, offering a more comprehensive approach to bone regeneration. Furthermore, the antimicrobial results surpass those of previous studies, demonstrating the exceptional efficacy of our treatment and highlighting its potential for infection control [24, 25].

The presence of closed pores in the treatment group highlights the intricate porosity, a key factor for bone regeneration. This finding aligns with the results reported by Szwed-Georgiou *et al.* [26]. Our study revealed a distinct pattern of bone formation, characterized by increased bone volume, surface area, and trabecular thickness in the treatment group, contrasting sharply with the control group. This deviation from the trends observed in previous studies further emphasizes the unique effectiveness of our approach [26, 27]. It is important to acknowledge that despite these affirmative results, further statistical validation is imperative to establish the robustness and significance of the observations. The rejection of the null hypothesis serves as a strong foundation for the potential clinical impact of our gelatin-based hydrogel in enhancing bone formation, laying the groundwork for future advancements in bone regenerative therapies.

A recent article explored novel tissue regeneration strategies, highlighting the significance of innovative biomaterials and bioactive molecules for bone repair. The parameters of our study align with this perspective, as we employ gelatin as a structural scaffold and incorporate quercetin and silver nanoparticles to enhance the biological properties of the hydrogel. This approach demonstrates compatibility with the evolving landscape of tissue engineering.

The work demonstrated by Wei *et al.* on bone tissue engineering using gelatin methacrylate (GelMA) hydrogel

and solid lipid nanoparticles (SLNs) loaded with resveratrol offers an understanding and insights into utilizing hydrogels for bone regeneration [27]. Although the focus of this article is on SLNs loaded with resveratrol, the study extends this concept by incorporating silver nanoparticles and quercetin, demonstrating a unique combination that contributes to enhanced bone formation potential. Moreover, a study by Abtahi *et al.* discusses Guided Bone Regeneration (GBR) using resorbable membranes [28]. While GBR primarily employs barrier membranes, this gelatin-based hydrogel serves as a three-dimensional scaffold with inherent properties beneficial for bone regeneration. The comparison enriches our understanding of various strategies within the domain of bone tissue engineering [29, 30, 31].

While the research shows promising results in enhancing bone formation with the injectable hydrogel, limitations include the reliance on an animal model and the need for extended observation periods to assess long-term effects. Clinically, the study addresses atrophic dental ridges with a minimally invasive approach, potentially improving implant success rates, as partially discussed in previous literature [32, 33, 5]. This technology also holds promise for other conditions involving bone defects. Future research could focus on optimizing the hydrogel formulation, exploring variations, conducting long-term human trials, and investigating synergistic approaches to further enhance bone regeneration.

CONCLUSION

The exploration of an injectable hydrogel containing quercetin and silver nanoparticles incorporated with gelatin presents promising avenues for enhancing bone formation, particularly in the challenging context of atrophic dental ridges and bone defects. While acknowledging limitations related to the animal model and the need for extended observations, the clinical significance is evident in offering a minimally invasive solution with potential implications for improved dental implant success rates. Future research focusing on optimizing the hydrogel formulation, conducting long-term human trials, and exploring synergistic approaches could further advance the field of bone tissue engineering. Overall, our findings contribute to addressing critical challenges in dental implantology and pave the way for innovative strategies in bone regeneration.

SUGGESTIONS FOR FUTURE RESEARCH

The authors of this study suggest investigating the effect of injectable hydrogel containing quercetin and silver nanoparticles with xenogenic silver nanoparticles for enhancing bone formations in humans.

AUTHORS' CONTRIBUTIONS

The authors confirm their contributions to the paper as follows: J.N.: Study conception and design; S.M.: Data Collection; K.G.M. and J.P.: Analysis and interpretation of results; D.R., G.M.: Draft manuscript; M.M.M.: Conceptualization; M.C.: Visualization. All authors reviewed the results and approved the final version of the manuscript.

LIST OF ABBREVIATIONS

ROS	=	Reactive Oxygen Species
DMSO	=	Dimethyl Sulfoxide
FBS	=	Fetal Bovine Serum
DFDBAs	=	Demineralized Freeze-Dried Bone Allografts
FDBAs	=	Freeze-Dried Bone Allografts

ETHICS APPROVAL AND CONSENT TO PARTICIPATE

This study was approved by the Ethics Committee of Saveetha Dental College, Saveetha Institute of Medical and Technical Sciences, India (BRULAC/SDCH/SIMATS/IAEC/05-2022/118).

HUMAN AND ANIMAL RIGHTS

The reported experiments in accordance with the standards set forth in CCSEA (Committee for Control and Supervision of Experiments on Animals) guidelines.

This study adheres to internationally accepted standards for animal research, following the 3Rs principle. The ARRIVE guidelines were employed for reporting experiments involving live animals, promoting ethical research practices.

CONSENT FOR PUBLICATION

Not applicable.

AVAILABILITY OF DATA AND MATERIALS

The data used to support the findings of this study were supplied by the corresponding author under license and data will be available on request.

FUNDING

None.

CONFLICT OF INTEREST

Dr. Giuseppe Minervini is the Co-EIC of the journal TODENTJ.

ACKNOWLEDGEMENTS

The authors would like to extend their gratitude to Saveetha Dental College and Hospital for their invaluable research support, with special thanks to Mr. Tebas and the White Lab for providing access to the Nano CT, Dr. Rajlaxmanan and his team at the Green Lab for material preparation, and Dr. Anand and the RED Lab team for animal handling.

REFERENCES

- [1] Zhao R, Yang R, Cooper PR, Khurshid Z, Shavandi A, Ratnayake J. Bone grafts and substitutes in dentistry: A review of current trends and developments. *Molecules* 2021; 26(10): 3007. <http://dx.doi.org/10.3390/molecules26103007> PMID: 34070157
- [2] Kumar P, Vinitha B, Fathima G. Bone grafts in dentistry. *J Pharm Bioallied Sci* 2013; 5(5) (Suppl. 1): 125. <http://dx.doi.org/10.4103/0975-7406.113312> PMID: 23946565
- [3] Ferraz MP. Bone grafts in dental medicine: An overview of autografts, allografts and synthetic materials. *Materials* 2023; 16(11): 4117. <http://dx.doi.org/10.3390/ma16114117> PMID: 37297251
- [4] Liang C, Ma L, Chen Y, *et al.* Artesunate alleviates kidney fibrosis in type 1 diabetes with periodontitis rats *via* promoting autophagy and suppression of inflammation. *ACS Omega* 2024; 9(14): 16358-73. <http://dx.doi.org/10.1021/acsomega.4c00020> PMID: 38617690
- [5] Al-Maula BH, Hussein BJ, Kadhim WA, *et al.* The effect of gold nanoparticles and apricot kernel extract on the osseointegration of dental implants - a rabbit model. *Open Dent J* 2024; 18(1): 18742106311522. <http://dx.doi.org/10.2174/0118742106311522240819071358>
- [6] Bow A, Anderson DE, Dhar M. Commercially available bone graft substitutes: The impact of origin and processing on graft functionality. *Drug Metab Rev* 2019; 51(4): 533-44. <http://dx.doi.org/10.1080/03602532.2019.1671860> PMID: 31577468
- [7] Smeets R, Stadlinger B, Schwarz F, *et al.* Impact of dental implant surface modifications on osseointegration. *BioMed Res Int* 2016; 2016: 1-16. <http://dx.doi.org/10.1155/2016/6285620> PMID: 27478833
- [8] Goyal S, Masood M, Le C, Rajendran Y, Nanjapa S, Vaderhobli R. Comparative bone graft evaluation for dental implant success: An evidence-based review. *J Long Term Eff Med Implants* 2021; 31(3): 33-44. <http://dx.doi.org/10.1615/JLongTermEffMedImplants.2021038292> PMID: 34369720
- [9] Cha HS, Kim JW, Hwang JH, Ahn KM. Frequency of bone graft in implant surgery. *Maxillofac Plast Reconstr Surg* 2016; 38(1): 19. <http://dx.doi.org/10.1186/s40902-016-0064-2> PMID: 27077072
- [10] de Azambuja Carvalho PH, dos Santos Trento G, Moura LB, Cunha G, Gabrielli MAC, Pereira-Filho VA. Horizontal ridge augmentation using xenogenous bone graft—systematic review. *Oral Maxillofac Surg* 2019; 23(3): 271-9. <http://dx.doi.org/10.1007/s10006-019-00777-y> PMID: 31089897
- [11] Schlegel AK, Donath K. BIO-OSS—a resorbable bone substitute? *J Long Term Eff Med Implants* 1998; 8(3-4): 201-9. PMID: 10186966
- [12] Malik R, Gupta A, Bansal P, Sharma R, Sharma S. Evaluation of alveolar ridge height gained by vertical ridge augmentation using titanium mesh and novabone putty in posterior mandible. *J Maxillofac Oral Surg* 2020; 19(1): 32-9. <http://dx.doi.org/10.1007/s12663-019-01250-9> PMID: 31988560
- [13] Alghamdi HS, van den Beucken JJJP, Jansen JA. Osteoporotic rat models for evaluation of osseointegration of bone implants. *Tissue Eng Part C Methods* 2014; 20(6): 493-505. <http://dx.doi.org/10.1089/ten.tec.2013.0327> PMID: 24124802
- [14] Nallaswamy D, Maiti S, Echhpal U, Shah KK, Raju L, Eswaramoorthy R. An *in vitro* study to evaluate the cell viability, surface characteristics, and osteoconductive potential of ovine bone graft modified with l-glutamine compared to commercial bone graft. *Int J Prosthodont Restor Dent* 2024; 14(3): 185-93. <http://dx.doi.org/10.5005/jp-journals-10019-1470>
- [15] Park H, Guo X, Temenoff JS, *et al.* Effect of swelling ratio of injectable hydrogel composites on chondrogenic differentiation of encapsulated rabbit marrow mesenchymal stem cells *in vitro*. *Biomacromolecules* 2009; 10(3): 541-6. <http://dx.doi.org/10.1021/bm801197m> PMID: 19173557
- [16] Kondiah P, Choonara Y, Kondiah P, *et al.* A review of injectable

- polymeric hydrogel systems for application in bone tissue engineering. *Molecules* 2016; 21(11): 1580.
<http://dx.doi.org/10.3390/molecules21111580> PMID: 27879635
- [17] George R, Maiti S, Ganapathy DM. Estimation of L-carnitine levels in diabetic completely edentulous patients for implant diagnosis: A cross-sectional study. *Dent Res J* 2023; 20(1): 96.
<http://dx.doi.org/10.4103/1735-3327.384367> PMID: 37810450
- [18] Badhwar R, Mangla B, Neupane YR, Khanna K, Popli H. Quercetin loaded silver nanoparticles in hydrogel matrices for diabetic wound healing. *Nanotechnology* 2021; 32(50): 505102.
<http://dx.doi.org/10.1088/1361-6528/ac2536> PMID: 34500444
- [19] Tsou YH, Khoneisser J, Huang PC, Xu X. Hydrogel as a bioactive material to regulate stem cell fate. *Bioact Mater* 2016; 1(1): 39-55.
<http://dx.doi.org/10.1016/j.bioactmat.2016.05.001> PMID: 29744394
- [20] El-Sherbiny IM, Yacoub MH. Hydrogel scaffolds for tissue engineering: Progress and challenges. *Glob Cardiol Sci Pract* 2013; 2013(3): 38.
<http://dx.doi.org/10.5339/gcsp.2013.38> PMID: 24689032
- [21] Karunakaran N, Maiti S, Jayaraman S, Paulraj J. Assessment of bone turnover markers prior to dental implant placement for osteoporosis patient- a case- control study. *Ann Dent Spec* 2023; 11(2-2023): 57-61.
<http://dx.doi.org/10.51847/Z8ruHjG41y>
- [22] Koppaka R, Shah KK, Maiti S. Multifaceted enhancement of l-leucine-enriched ovine bone graft: Physicochemical characteristics and osteogenic potential for improved guided bone regeneration. *Cureus* 2024; 16(7): 64416.
<http://dx.doi.org/10.7759/cureus.64416> PMID: 39131038
- [23] Han X, He J, Wang Z, *et al.* Fabrication of silver nanoparticles/gelatin hydrogel system for bone regeneration and fracture treatment. *Drug Deliv* 2021; 28(1): 319-24.
<http://dx.doi.org/10.1080/10717544.2020.1869865> PMID: 33517806
- [24] Ahmad N, Fozia , Jabeen M, *et al.* Green fabrication of silver nanoparticles using *euphorbia serpens* kunth aqueous extract, their characterization, and investigation of its *in vitro* antioxidative, antimicrobial, insecticidal, and cytotoxic activities. *BioMed Res Int* 2022; 2022(1): 5562849.
<http://dx.doi.org/10.1155/2022/5562849> PMID: 35047637
- [25] Costa-Pinto AR, Reis RL, Neves NM. Scaffolds based bone tissue engineering: The role of chitosan. *Tissue Eng Part B Rev* 2011; 17(5): 331-47.
<http://dx.doi.org/10.1089/ten.teb.2010.0704> PMID: 21810029
- [26] Szwed-Georgiou A, Płociński P, Kupikowska-Stobba B, *et al.* Bioactive materials for bone regeneration: Biomolecules and delivery systems. *ACS Biomater Sci Eng* 2023; 9(9): 5222-54.
<http://dx.doi.org/10.1021/acsbiomaterials.3c00609> PMID: 37585562
- [27] Wei B, Wang W, Liu X, *et al.* Gelatin methacrylate hydrogel scaffold carrying resveratrol-loaded solid lipid nanoparticles for enhancement of osteogenic differentiation of BMSCs and effective bone regeneration. *Regen Biomater* 2021; 8(5): rbab044.
<http://dx.doi.org/10.1093/rb/rbab044> PMID: 34394955
- [28] Abtahi S, Chen X, Shahabi S, Nasiri N. Resorbable membranes for guided bone regeneration: Critical features, potentials, and limitations. *ACS Mater Au* 2023; 3(5): 394-417.
<http://dx.doi.org/10.1021/acsmaterialsau.3c00013> PMID: 38089090
- [29] Wang J, Wu Y, Li G, *et al.* Engineering large-scale self-mineralizing bone organoids with bone matrix-inspired hydroxyapatite hybrid bioinks. *Adv Mater* 2024; 36(30): 2309875.
<http://dx.doi.org/10.1002/adma.202309875> PMID: 38642033
- [30] Lin CH, Srioudom JR, Sun W, *et al.* The use of hydrogel microspheres as cell and drug delivery carriers for bone, cartilage, and soft tissue regeneration. *Biomater Transl* 2024; 5(3): 236-56.
<http://dx.doi.org/10.12336/biomatertransl.2024.03.003> PMID: 39734701
- [31] Lu P, Ruan D, Huang M, *et al.* Harnessing the potential of hydrogels for advanced therapeutic applications: Current achievements and future directions. *Signal Transduct Target Ther* 2024; 9(1): 166.
<http://dx.doi.org/10.1038/s41392-024-01852-x> PMID: 38945949
- [32] Rupawat D, Maiti S, Nallaswamy D, Sivaswamy V. Aesthetic outcome of implants in the anterior zone after socket preservation and conventional implant placement: A retrospective study. *J Long Term Eff Med Implants* 2020; 30(4): 233-9.
<http://dx.doi.org/10.1615/JLongTermEffMedImplants.2020035942> PMID: 33463922
- [33] Rajaraman V, Nallaswamy D, Ganapathy DM, Kachhara S. Osseointegration of hafnium when compared to titanium - a structured review. *Open Dent J* 2021; 15(1): 137-44.
<http://dx.doi.org/10.2174/1874210602115010137>

DISCLAIMER: The above article has been published, as is, ahead-of-print, to provide early visibility but is not the final version. Major publication processes like copyediting, proofing, typesetting and further review are still to be done and may lead to changes in the final published version, if it is eventually published. All legal disclaimers that apply to the final published article also apply to this ahead-of-print version.